

1 *An assessment of the role of the k-ε vertical mixing scheme in the simulation* 2 *of Southern Ocean upper dynamics*

3 Kirodh Boodhraj^{1,2,*}, Marcello Vichi^{2,3} and Jacoba E. Smit¹

4 ¹CSIR Modelling and Digital Science, Advanced Mathematical Modelling, Stellenbosch 7600, South Africa

5 ²Dept. of Oceanography, University of Cape Town, Rondebosch 7701, Cape Town, South Africa

6 ³Marine Research Institute, University of Cape Town, Rondebosch 7701, Cape Town, South Africa

7 Following the work done by Reffrey, Calone and Bourdalle-Badie (2015) we implemented a one
8 dimensional(1D) ocean physical model in the sub-Antarctic Southern Ocean using the Nucleus for the
9 European Modelling of the Ocean(NEMO) model. The 1D model is a first attempt at studying sub-grid scale
10 parameterizations in the region. It was used to test the effects of the k-ε turbulence closure scheme on the
11 simulation of vertical mixing in the water column structure in the North Pacific and Southern Ocean, using the
12 available scattered data as comparison. This analysis also gives indications for the choice of the grid's vertical
13 levels.

14
15 **Keywords:** NEMO, Sub-mesoscale Parameterizations, Turbulence Closure Model, Vertical Mixing, Southern
16 Ocean

17 *Introduction*

18 Currently the first African based Earth System
19 model, the Variable Resolution Earth Systems
20 Model (VRESM), is being developed at the
21 CSIR and will greatly enhance understanding
22 regional effects of climate change. Many
23 components of the model that were optimized
24 for other locations need to be adapted and
25 optimized before the model can be implemented
26 with focus on the African continent. One of the
27 model components is the use of sub-grid scale
28 parameterization techniques (Gent and
29 McWilliams, 1990; Fox-Kemper et al., 2008) to
30 resolve eddies.

31
32 The initial step to achieve this relies on vertical
33 mixing processes. In a general model of the
34 ocean, the choice of the vertical mixing model is
35 essential to achieve more accurate modelling
36 results. The vertical mixing will cause density
37 differences that will result in the stratification of
38 the water column which shifts the thermocline
39 and halocline according to season. This physical
40 process is important for marine species survival.

41
42 The objective of this paper is the use of vertical
43 turbulence closure schemes to model vertical
44 mixing processes similar to Reffray et al. (2015).
45 Furthermore, Southern Ocean (SO) conditions
46 were applied to find the temperature and salinity
47 results for 75 and 51 vertical levels.

49 *Instrumentation and Method*

50 Reffray et al. (2015) concentrated on comparing
51 the results of using different vertical turbulence
52 models that come with NEMO
53 (<http://www.nemo-ocean.eu>; Madec et al., 2016)

54 to observed data in the ocean. The k-ε turbulence
55 model (Versteeg and Malalasekera, 2007) was
56 used in this paper because Reffray et al. (2015)
57 concluded that this model produced the most
58 accurate results in comparison to the other
59 turbulence models.

60
61 Reffray et al. (2015) used a 1-dimensional code
62 referred to as the C1D_PAPA case to test the
63 different turbulence schemes. The initial and
64 boundary conditions files are included with
65 C1D_PAPA. This case was later tailored to use
66 SO conditions. C1D_PAPA uses an Arakawa A
67 grid type consisting of a column composed of a
68 3×3 horizontal grid (x- and y-directions) with an
69 ideal resolution of 0.1° × 0.1° with 75 vertical
70 levels (z-direction). All the 9 water columns are
71 identical and allow removing horizontal
72 processes by zeroing the gradients while keeping
73 the same computer code structure i.e. the 9
74 columns are needed only for the sound operation
75 of NEMO but every level has the same
76 temperature, salinity, velocity etc. values. The
77 time step used was set to 360 s.

78
79 The observed data (needed for comparison with
80 the calculated results) from PAPA Station was
81 obtained from the National Ocean Atmospheric
82 Administration (NOAA, 2016) website. The
83 PAPA Station is located in the North Pacific
84 Ocean. The SO station was ideally located in the
85 sub-Antarctic zone at 46S, 4W. The initial
86 conditions were obtained from the World Ocean
87 Atlas (Locarnini et al., 2013) and the forcing
88 data from European Centre for Medium-Range
89 Weather Forecasts (ECMWF) ERA-interim
90 reanalysis (Dee et al., 2011).

*Email: kboodhraj@csir.co.za,
Office number: +27 21 888 2501
Fax number: +27 21 888 2693

91 Reffray et al. (2015) calculated the bias for the
 92 temperature by subtracting the calculated data
 93 from the observed data. All plots, for the North
 94 Pacific and SO, were plotted for the period
 95 15 June 2010 to 14 June 2011 unless otherwise
 96 stated.

97
 98 The following density model was chosen to
 99 calculate the density (Millero and Poisson, 1981)
 100 using the output from NEMO:

$$\rho(T, S) = AS + BS^{1.5} + CS^2 \quad (1)$$

101 ,where

$$\begin{aligned} A(T) = & 8.24493 \times 10^{-1} \quad (2) \\ & - 4.0899 \times 10^{-3}T \\ & + 7.6438 \times 10^{-5}T^2 \\ & - 8.2467 \times 10^{-7}T^3 \\ & + 5.3875 \times 10^{-9}T^4 \end{aligned}$$

$$\begin{aligned} B(T) = & -5.72466 \times 10^{-3} \quad (3) \\ & + 1.0227 \times 10^{-4}T \\ & - 1.6546 \times 10^{-6}T^2 \end{aligned}$$

$$C(T) = 4.8314 \times 10^{-4} \quad (4)$$

102 ,where ρ is the density, T the temperature and S
 103 the salinity. Note that the density is a function of
 104 salinity and temperature only.

105
 106 The Root Mean Square Error (RMSE) for the
 107 temperature was calculated using the standard
 108 formula:

$$RMSE = \sqrt{\frac{\sum_{i=1}^n (T_i^{Comp} - T_i^{Obs})^2}{n}} \quad (5)$$

109

110 **Results and Discussion**

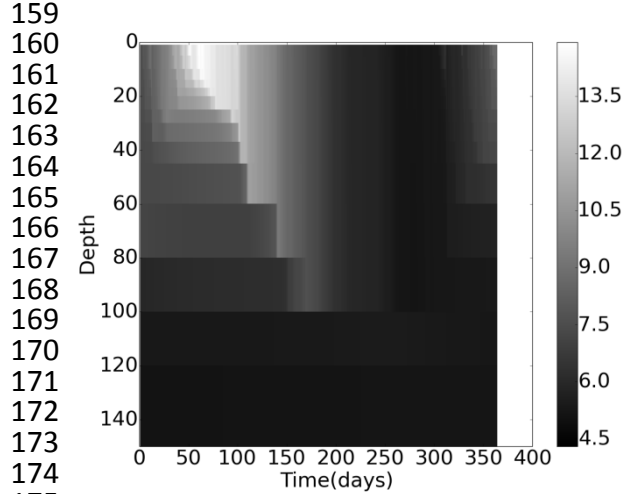
111 Results following Reffray et al. (2015) work are
 112 shown in Figs. 1-3. Results following Figs. 4-7
 113 were independent of Reffray et al. (2015).

114
 115 Both the temperature data in Fig. 1 and the
 116 temperature bias in Fig. 2 show that within the
 117 first five months there was a large stratification
 118 with a shallow Mixed Layer Depth (MLD)
 119 within a depth of 0 – 60 m. The high bias within
 120 the first five months indicated that the model
 121 could not represent the observed data accurately.
 122 The reason being that the MLD was shallower
 123 during the summer because of the surface
 124 heating. Seasonal surface cooling then destroyed
 125 the stratification for the rest of the year which
 126 deepened the MLD and caused the homogeneity.
 127 The bias (Fig. 2), found from the distribution of
 128 the calculated and observed temperature,
 129 followed the same trend as what Reffray et al.

130 (2015) had found. The main difference was that
 131 the calculated temperature RMSE values (Fig. 3)
 132 were higher than what Reffray et al. (2015) had
 133 found.

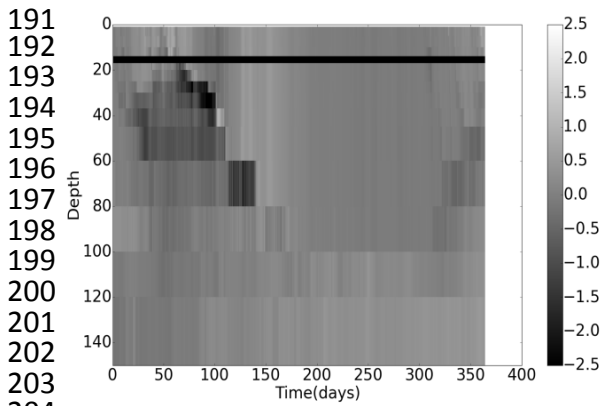
134
 135 The temperature RMSE values stabilized from
 136 midyear to the end of the year to 0.15 ± 0.05 °C.
 137 Reffray et al. (2015) RMSE values stabilized to
 138 0.05 ± 0.3 °C. The discrepancy could have arisen
 139 from the averaging of data to obtain the biases as
 140 Reffray et al. (2015) had calculated the RMSE
 141 values up to 120 m whereas in this paper the
 142 RMSE's were calculated up to 300 m. The
 143 reason for calculating the RMSE up to 300 m
 144 was to take into account the MLD
 145 (homogeneous region) which extends lower than
 146 120 m.

147
 148 The results for the density (calculated using
 149 Eqs. 7–10) are shown in Figs. 4 and 5. The
 150 calculated densities lie within an error of
 151 ± 0.5 kg/m³ from the observed values. The
 152 overall form of the graphs for both September
 153 (during the mixing period) and October (the
 154 beginning of the mixing period) are similar to
 155 the observed data. The depth of the pycnocline
 156 suddenly increased in October, because of the
 157 seasonal change which started the mixing in
 158 autumn.

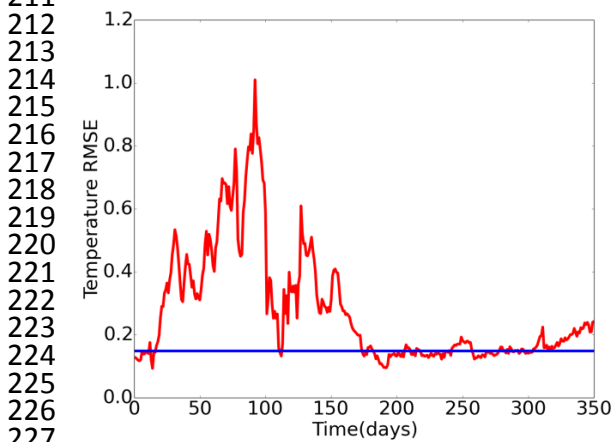


160
 161
 162
 163
 164
 165
 166
 167
 168
 169
 170
 171
 172
 173
 174
 175
 176 **Figure 1:** The calculated temperature for the period
 177 15 June 2010 to 14 June 2011 using the NEMO
 178 C1D_PAPA case. The k-ε model was used with a time
 179 step of 360 s.

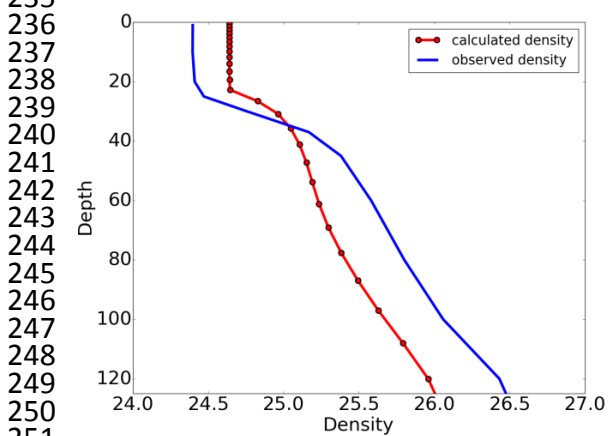
180
 181 The results for temperature and salinity using SO
 182 conditions are shown in Figs. 6 and 7. In both
 183 the temperature and salinity calculated data the
 184 surface fluxes influenced the upper 300 m of the
 185 stratified water column. In the upper layer of Fig.
 186 6, the temperature slowly increased and then
 187 decreased as time progressed. In the upper layer
 188 of Fig. 7, the salinity continually decreased as
 189 time progressed, indicating a drift likely due to
 190 the one-dimensional approximation.



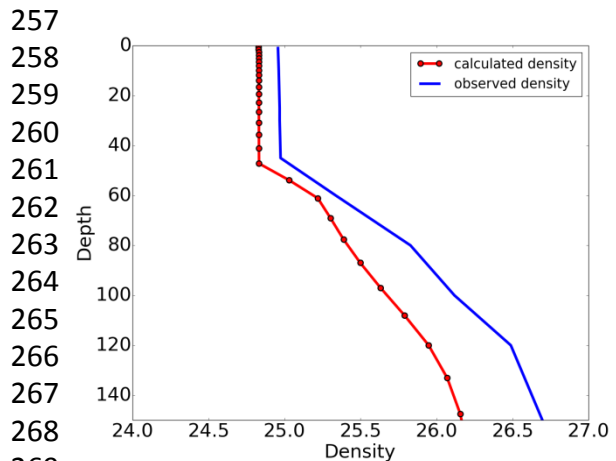
191
192
193
194
195
196
197
198
199
200
201
202
203
204
205 **Figure 2:** The temperature bias for the period
206 15 June 2010 to 14 June 2011 using the calculated
207 data from NEMO C1D_PAPA case and the observed
208 data from PAPA Station. The k-ε model was used
209 with a time step of 360 s. There was no observed
210 data for the horizontal band around 15 m.
211



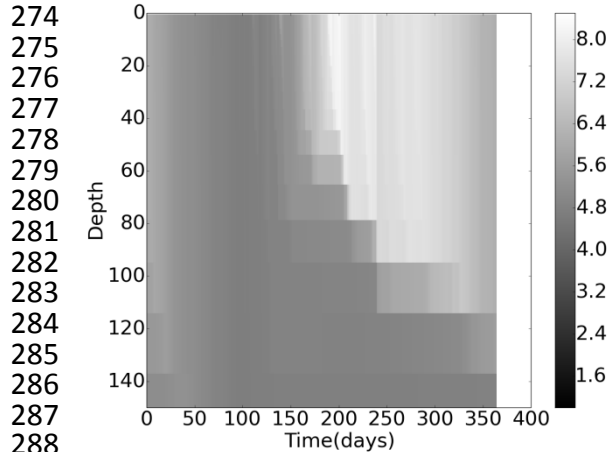
212
213
214
215
216
217
218
219
220
221
222
223
224
225
226
227
228 **Figure 3:** The temperature RMSE calculation for the
229 period 15 June 2010 to 14 June 2011 using the
230 calculated data from NEMO C1D_PAPA case and the
231 observed data from PAPA Station. The horizontal line
232 indicates that the RMSE stabilized to 0.15 °C. The k-ε
233 model was used with a time step of 360 s.
234



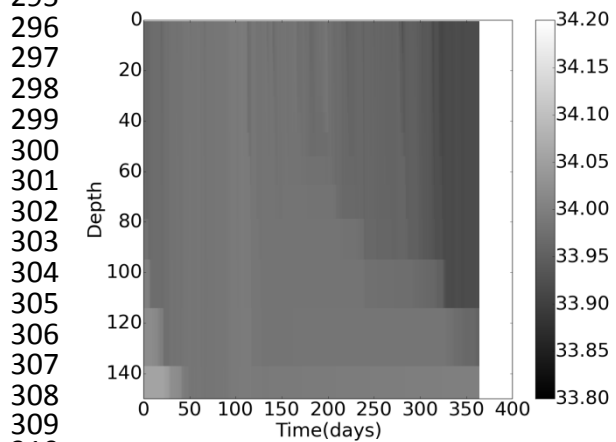
235
236
237
238
239
240
241
242
243
244
245
246
247
248
249
250
251
252 **Figure 4:** The density calculation for
253 12 September 2010 (during mixing period) using
254 the calculated data from NEMO C1D_PAPA case
255 compared to the observed data from PAPA Station.
256



257
258
259
260
261
262
263
264
265
266
267
268
269
270 **Figure 5:** The density calculation for 12 October 2010
271 (beginning of mixing period) using the calculated data
272 from NEMO C1D_PAPA case compared to the
273 observed data from PAPA Station.
274



275
276
277
278
279
280
281
282
283
284
285
286
287
288
289 **Figure 6:** The calculated temperature for the period
290 15 June 2010 to 14 June 2011 using SO conditions
291 produce the same result for 51 and 75 vertical levels.
292 The k-ε model was used with a time step of 360 s.
293



294
295
296
297
298
299
300
301
302
303
304
305
306
307
308
309
310
311 **Figure 7:** The calculated salinity for the period
312 15 June 2010 to 14 June 2011 using SO conditions
313 produce the same result for 51 and 75 vertical levels.
314 The k-ε model was used with a time step of 360 s.

315 A grid sensitivity test for the SO model was done
316 by changing the number of vertical levels from
317 75 to 51. The temperature and salinity results
318 were the same as Figs. 6 and 7 with no apparent
319 changes in the structures.

320
321 Future work will include the modification of
322 C1D_PAPA to verify the results of the other
323 turbulence closure schemes (Turbulent Kinetic
324 Energy (TKE), k-kl, k- ω and Generic). There is
325 scope to test the vertical grid sensitivity further
326 i.e. increase the number of vertical levels to
327 assess whether vertical mixing is affected. Mixed
328 layer depths in the region are usually deeper than
329 150 m and it is worth assessing whether a 1D
330 model can reproduce them purely through local
331 turbulence. The SO has a stronger horizontal
332 advection which may influence the results and
333 therefore it may also be necessary to consider
334 restoration to avoid drifts as seen for salinity.

335 336 **Conclusions**

337 This paper highlights the first attempt to study
338 the vertical mixing in the SO using NEMO. The
339 results obtained from Figs. 1-3 were found from
340 following Reffray et al. (2015) and the results
341 from Figs 4-7 were found from applying SO
342 conditions to the tailored C1D_PAPA case. The
343 RMSE values converged within the time period
344 however the value was approximately 0.1 °C
345 bigger than what Reffray et al. (2015) had found.
346 The density model (Eqs. 7-10) produced results
347 within an error margin of 0.5 kg/m³ and also
348 had a similar form to the observed data. Using
349 SO conditions and changing the vertical levels to
350 51, it was found that the temperature and salinity
351 results (Figs. 6 and 7) were identical compared
352 to having 75 vertical levels. Scope lies within
353 investigating the results of increasing the number
354 of vertical levels and implementing other
355 turbulence models using SO conditions.

356 357 **Acknowledgements**

358 The present work is funded by the CSIR
359 Parliamentary Grant and the VRESM SRP
360 project from Prof. Francois Engelbrecht.
361 Acknowledgement is given to Dr Björn
362 Backeberg for funding this extended abstract.

363 364 **References**

365 (i) Journals:
366 Reffray, G., Bourdalle-Badie, R. and
367 Calone, C. (2015). Modelling turbulent
368 vertical mixing sensitivity using a 1-D
369 version of NEMO. *Geoscientific Model*
370 *Development*. 8: 69-86
371 Gent, P.R. and McWilliams, J.C. (1990).
372 Isopycnal mixing in ocean circulation
373 models. *Journal of Physical*

374 *Oceanography*. 20:150–155
375 Fox-Kemper, B., Ferrari, R. and Hallberg,
376 R. (2008). Parameterization of mixed
377 layer eddies. Part I: Theory and diagnosis.
378 *Journal of Physical Oceanography*. 38(6):
379 1145-1165
380 Millero, F. J. and Poisson, A. (1981).
381 International one-atmosphere equation of
382 state of seawater. *Deep-Sea Research*,
383 *Elsevier*. 6: 625-629
384 Dee, D. P., Uppala, S. M., Simmons, A. J.,
385 Berrisford, P., Poli, P., Kobayashi, S.,
386 Andrae, U., Balmaseda, M. A., Balsamo,
387 G., Bauer, P., Bechtold, P., Beljaars, A. C.
388 M., van de Berg, L., Bidlot, J., Bormann,
389 N., Delsol, C., Dragani, R., Fuentes, M.,
390 Geer, A. J., Haimberger, L., Healy, S. B.,
391 Hersbach, H., Hólm, E. V., Isaksen, I.,
392 Kållberg, P., Köhler, M., Matricardi, M.,
393 McNally, A. P., Monge-Sanz, B.M.,
394 Morcrette, J. J., Park, B. K., Peubey, C., de
395 Rosnay, P., Tavolato, C., Thépaut, J. N.,
396 Vitart, F., (2011). The ERA-Interim
397 reanalysis: configuration and performance
398 of the data assimilation system. *Quarterly*
399 *Journal of the Royal Meteorological*
400 *Society*. 137(656): 553–597
401 Locarnini, R. A., Mishonov, A. V., Antonov,
402 J. I., Boyer, T. P., Garcia, H. E., Baranova,
403 O. K., Zweng, M. M., Paver, C. R.,
404 Reagan, J. R., Johnson, D. R., Hamilton,
405 M. and Seidov, D. (2013). World Ocean
406 Atlas (2013). Volume 1: Temperature.
407 Levitus, S. Ed., Mishonov, A. Technical
408 Ed.; *NOAA Atlas NESDIS*. 73:40.

409 410 (ii) Books:

411 Madec, G. and the NEMO team (2016).
412 *NEMO ocean engine*, Note du Pole de
413 modelisation de l'Institut Pierre-Simon
414 Laplace No 27.
415 Cushman-Rosin, B. and Beckers, J.-M.
416 (2009). *Introduction to Geophysical Fluid*
417 *Dynamics: Physical and Numerical*
418 *Aspects*, Academic Press.
419 Versteeg, H. and Malalasekera, W. (2007). *An*
420 *Introduction to Computational Fluid*
421 *Dynamics: The Finite Volume Method*,
422 Pearson.

423 424 (iii) Web references:

425 Arrigo, K. (2002). Lecture 3: Temperature,
426 Salinity, Density and Ocean Circulation.
427 [http://ocean.stanford.edu/courses/bomc/ch](http://ocean.stanford.edu/courses/bomc/chem/lecture_03.pdf)
428 [em/lecture_03.pdf](http://ocean.stanford.edu/courses/bomc/chem/lecture_03.pdf). Last accessed July
429 2016.
430 NOAA, 2016, *Ocean Station Papa*,
431 <http://www.pmel.noaa.gov/ocs/Papa>. Last
432 accessed July 2016.